

SCIENTIFIC REPORTS

OPEN

Temperature dependent local atomic displacements in ammonia intercalated iron selenide superconductor

Received: 31 March 2016

Accepted: 19 May 2016

Published: 09 June 2016

E. Paris^{1,2}, L. Simonelli³, T. Wakita^{4,5,†}, C. Marini³, J.-H. Lee⁶, W. Olszewski^{3,7}, K. Terashima^{4,5,†}, T. Kakuto⁶, N. Nishimoto⁶, T. Kimura⁶, K. Kudo^{5,6,†}, T. Kambe⁶, M. Nohara^{5,6,†}, T. Yokoya^{4,5,†} & N. L. Saini¹

Recently, ammonia-thermal reaction has been used for molecular intercalation in layered FeSe, resulting a new $\text{Li}_x(\text{NH}_3)_y\text{Fe}_2\text{Se}_2$ superconductor with $T_c \sim 45$ K. Here, we have used temperature dependent extended x-ray absorption fine structure (EXAFS) to investigate local atomic displacements in single crystals of this new superconductor. Using polarized EXAFS at Fe K-edge we have obtained direct information on the local Fe-Se and Fe-Fe bondlengths and corresponding mean square relative displacements (MSRD). We find that the Se-height in the intercalated system is lower than the one in the binary FeSe, suggesting compressed FeSe_4 tetrahedron in the title system. Incidentally, there is hardly any effect of the intercalation on the bondlengths characteristics, revealed by the Einstein temperatures, that are similar to those found in the binary FeSe. Therefore, the molecular intercalation induces an effective compression and decouples the FeSe slabs. Furthermore, the results reveal an anomalous change in the atomic correlations across T_c , appearing as a clear decrease in the MSRD, indicating hardening of the local lattice mode. Similar response of the local lattice has been found in other families of superconductors, e.g., A15-type and cuprates superconductors. This observation suggests that local atomic correlations should have some direct correlation with the superconductivity.

Among iron-based layered superconductors, the binary FeSe system with PbO-type structure¹ is apparently the simplest system without any spacer layers, that may represent the multiband electronic structure of these materials. The superconducting transition temperature of the binary FeSe is ~ 8 K and it can be increased by anion substitution in the ternary $\text{FeSe}_{1-x}\text{Te}_x$, showing a maximum T_c of ~ 15 K. The binary FeSe seems to offer less chemical flexibility than the others because of the lack of any spacers between the active FeSe layers, however, the T_c of FeSe increases sharply to ~ 37 K² under the high hydrostatic pressure, a clear hope to manipulate it further. A promising way to increase T_c is the introduction of chemical strain by intercalation of the FeSe layers. Indeed, the binary FeSe was successfully intercalated by alkaline atoms for matching the chemical pressure to the physical pressure, resulting in the discovery of $\text{A}_x\text{Fe}_{2-y}\text{Se}_2$ ($\text{A} = \text{K}, \text{Cs}, \text{Tl}$) materials with a T_c of ~ 32 K^{3,4}. The alkaline atom intercalated system is interesting due to its peculiar microstructural properties in which the superconducting quantum state is embedded in a Mott insulating state characterized by a large magnetic moment⁵, however, its complexity hardly helps to go beyond.

Recently, ammonia-thermal reaction has permitted a simultaneous intercalation of lithium cations, amide anions and ammonia molecules between the FeSe layers, producing $\text{Li}_x(\text{NH}_3)_y\text{Fe}_2\text{Se}_2$ superconductor with T_c

¹Dipartimento di Fisica, Sapienza Università di Roma, P. le Aldo Moro 2, 00185 Roma, Italy. ²Center for Life NanoScience@Sapienza, Istituto Italiano di Tecnologia, V. le Regina Elena 291, 00185 Rome, Italy. ³ALBA Synchrotron Light Facility, Carrer de la Llum 2-26, 08290 Cerdanyola del Vallés, Barcelona, Spain. ⁴Research Laboratory for Surface Science, Okayama University, Okayama 700-8530, Japan. ⁵Research Centre of New Functional Materials for Energy Production, Storage and Transport, Okayama University, Okayama 700-8530, Japan. ⁶Department of Physics, Okayama University, Kita-ku, Okayama 700-8530, Japan. ⁷Faculty of Physics, University of Białystok, 1L K. Ciokowskiego Str., 15-245 Białystok, Poland. [†]Present address: Research Institute for Interdisciplinary Science, Okayama University, Okayama 700-8530, Japan. Correspondence and requests for materials should be addressed to N.L.S. (email: Naurang.Saini@roma1.infn.it)

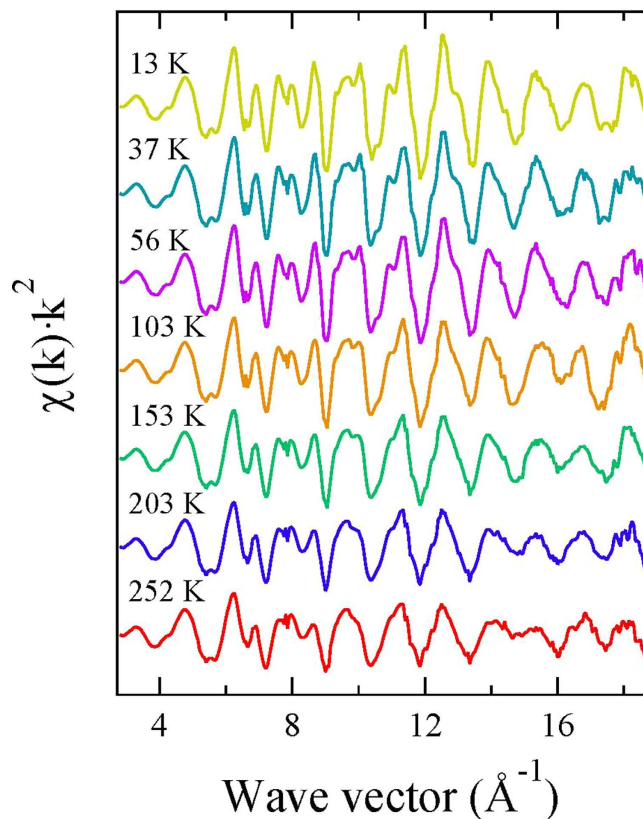


Figure 1. Temperature evolution of the EXAFS oscillations (k^2 -weighted) extracted from in-plane polarized Fe K-edge x-ray absorption spectra measured on single crystal sample of $\text{Li}_x(\text{NH}_3)_y\text{Fe}_2\text{Se}_2$ system. The EXAFS oscillations are shown vertically shifted for a better visualization.

depending on the thickness of the intercalated spacer layer (maximum $T_c \sim 45 \text{ K}$)^{6–13}. Unlike $\text{A}_x\text{Fe}_{2-y}\text{Se}_2$ compounds, the new system with molecular spacer layer intercalation is crystallographically homogeneous, however, little is known about its local structure. The physical parameters, which are likely to have major role in the superconducting state, are generally controlled by strain/stress fields due to interlayer interactions. For example, when the binary FeSe is produced as a monolayer grown on SrTiO_3 the T_c increases upto $\sim 100 \text{ K}$ ¹⁴. This notable experimental result further confirms that local physics and defect chemistry is playing a central role in the superconducting mechanism. Indeed, iron-based superconductors are multiband systems with the electronic properties highly susceptible to any small disorder¹⁵ affecting the local structural parameters^{16,17}, e.g., the bond angle and the anion height from the Fe-Fe layer. In this context it is important to understand what is the response of the local structure to the intercalation of the molecular spacer layer and superconductivity of the intercalated system. In this work, we have addressed some of these issues and studied the local structure of ammonia intercalated $\text{Li}_x(\text{NH}_3)_y\text{Fe}_2\text{Se}_2$ by means of temperature-dependent x-ray absorption spectroscopy. We have exploited polarization dependence of the absorption cross-section to have direct access to the near-neighbour distances in single crystal samples of $\text{Li}_x(\text{NH}_3)_y\text{Fe}_2\text{Se}_2$ using extended x-ray absorption fine structure (EXAFS) measurements performed at the Fe K-edge.

Here, the focus is on the in-plane polarized x-ray absorption measurements providing direct access to both Fe-Se and Fe-Fe atomic correlations. Figure 1 shows (k^2 -weighted) EXAFS oscillations extracted from the in-plane polarized Fe K-edge x-ray absorption spectra measured at several temperatures. The EXAFS oscillations are visible upto high wave vector (k) above the noise level and show clear evolution as a function of temperature. Apart from a thermal damping, the EXAFS oscillations also reveal apparent structural changes (see, e.g., k -range $8\text{--}10 \text{ \AA}^{-1}$), indicating change in the local structure as a function of temperature. Such changes can be better visualized in the Fourier transform (FT) of EXAFS oscillations, displayed in Fig. 2. The FT magnitudes of EXAFS oscillations provide atomic distribution around the selected atomic site. Therefore, in the Fe K-edge EXAFS the axis origin is placed at the photon-absorbing Fe site while the scatterings with neighbouring atoms appear as peaks in the R -space. The FT are not corrected for the scattering phase-shifts and hence the peaks do not appear at the actual distances from Fe. The double peak structure between 1.5 and 3 \AA is due to Fe-Se pair (distance $\sim 2.4 \text{ \AA}$) and Fe-Fe pair (distance $\sim 2.7 \text{ \AA}$). The peaks appearing at longer distances are due to single scattering contributions of distant shells and multiple scatterings involving different paths, i.e., Fe-Fe (distance $\sim 3.8 \text{ \AA}$) and multiple scatterings involving Fe-Se (distance $\sim 4.8 \text{ \AA}$), Fe-Fe (distance $\sim 5.3 \text{ \AA}$) and Fe-Fe (distance $\sim 5.8 \text{ \AA}$). The high quality of EXAFS data can be judged from both EXAFS and FT amplitudes, revealing a systematic temperature evolution.

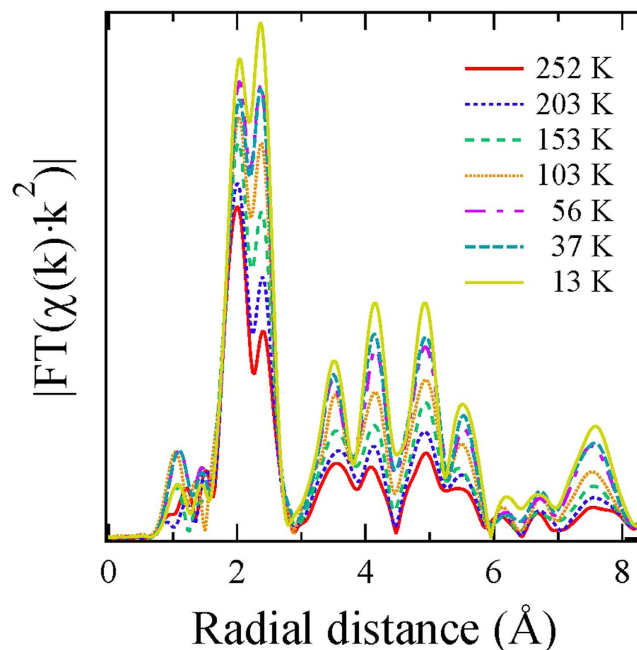


Figure 2. Temperature evolution of Fourier transform (FT) of the EXAFS oscillations measured on $\text{Li}_x(\text{NH}_3)_y\text{Fe}_2\text{Se}_2$ system. The FTs are performed in the k -range $3\text{--}17 \text{ \AA}^{-1}$ using a sine-shaped window.

In order to obtain the local structural parameters we have modeled the EXAFS signal using the equation based on single scattering approximation¹⁸:

$$\chi(k) = \sum_i \frac{N_i S_0^2}{k R_i^2} f_i(k, R_i) e^{-\frac{2R_i}{\lambda}} e^{-2k^2 \sigma_i^2} \sin(2kR_i + \delta_i(k)) \quad (1)$$

where N_i is the number of neighbouring atoms at a distance R_i , δ_i is the phase shift, $f_i(k, R_i)$ is the back-scattering amplitude, λ is the photoelectron mean free path and σ_i^2 is the EXAFS Debye-Waller factor measuring the mean square relative displacements (MSRD) of the photoabsorber-backscatter pairs. The S_0^2 is the so-called passive electrons reduction factor, i.e. EXAFS amplitude reduction factor due to many-body effects related with the losses occurring during the photoelectron propagation in the material (excitations as plasmons, electronhole pairs, etc) and the intrinsic losses due to shake-up and shake-off excitations created by the core-hole in the absorption process. The EXAFS modelling has been carried out by the Artemis package¹⁹ that uses the FEFF8 code²⁰ for the phase and amplitude functions. As a starting structure model we have used tetrahedrally coordinated FeSe taken from the known diffraction results⁶. In the structure, the first coordination shell is composed of 4 Se atoms (at a distance $\sim 2.4 \text{ \AA}$) and the second shell is composed of 4 Fe atoms (at a distance $\sim 2.7 \text{ \AA}$). The effect of beam polarization (since single crystal samples are used) has been taken into account by introducing an *effective* number of neighbors considering projections of the bond with respect to polarization vector of the x-ray beam. The S_0^2 is fixed after the analysis of five different EXAFS scans, providing S_0^2 to be 0.5. In the two shells model fits, 5 parameters were floated, i.e., two bond distances (Fe-Se and Fe-Fe), two corresponding σ^2 and the photoelectron energy zero (E_0). The latter was initially set to 2.5 eV after analyzing different scans at a constant temperature and floated within $\pm 1 \text{ eV}$ in subsequent fits to get the best fits at all temperatures. The k -range for the model fits was $3\text{--}17 \text{ \AA}^{-1}$ while the R -range was $1.5\text{--}3.0 \text{ \AA}$, providing the number of independent data points²¹ $2\Delta k\Delta R/\pi$ to be ~ 13 . Figure 3 shows examples of the two shells model fits (solid lines) in which 5 parameters were allowed to vary.

Figure 4 shows temperature dependence of the local Fe-Se and Fe-Fe bond distances. While the Fe-Se distance tends to increase with temperature (maximum $\Delta R \sim 0.005 \text{ \AA}$), the Fe-Fe distance remains basically temperature independent. The anion height from the Fe-Fe layer and the associated bond angle have been proposed to be the key parameters for superconductivity in iron-based materials, having a direct relationship with T_c ¹⁶. The present measurements permit to determine these parameters from the measured bondlengths. Assuming tetrahedral coordination of Se we can determine the Se height (h_z) and Se-Fe-Se bond angle (α) using the following relations:

$$h_z = \sqrt{R_{\text{Fe-Se}}^2 - \frac{1}{2}R_{\text{Fe-Fe}}^2}$$

$$\alpha = \pi - 2 \cos^{-1} \left(\frac{R_{\text{Fe-Fe}}}{\sqrt{2}R_{\text{Fe-Se}}} \right) \quad (2)$$

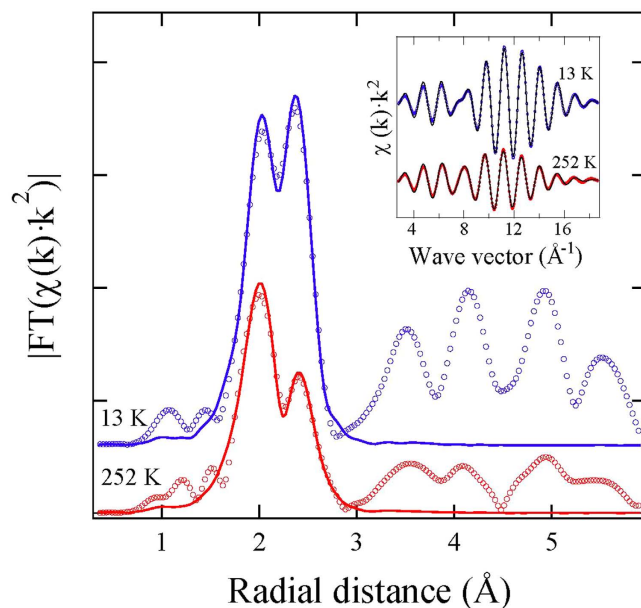


Figure 3. Fourier transforms of $\chi(k) \cdot k^2$ at two temperatures (empty circles), shown along with the two shells model fits (solid line). The inset shows the respective back Fourier filtered EXAFS oscillations with model fits (R-interval 1.5–3.0 Å).

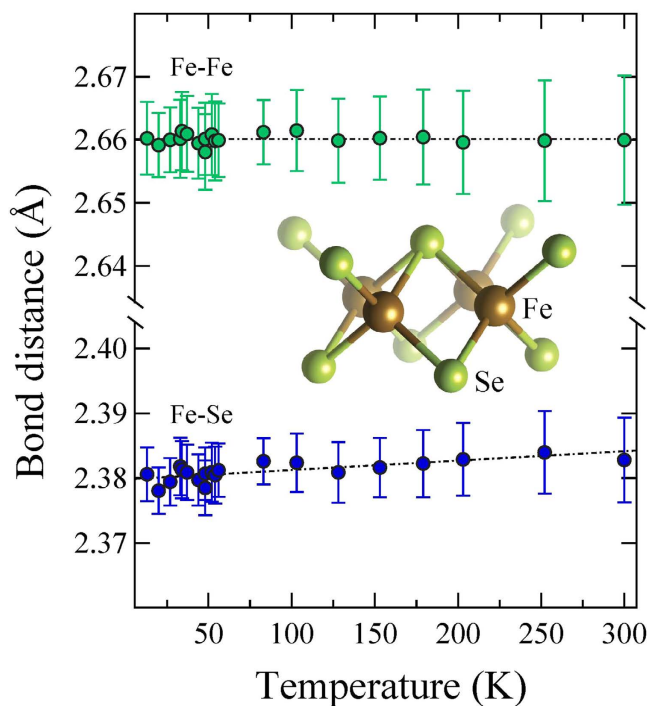


Figure 4. Temperature dependence of the local Fe-Se and Fe-Fe distances obtained from the least-squares fitting of the in-plane polarized Fe K-edge EXAFS oscillations. Inset shows a sketch of the local coordination environment around Fe atom. The dashed line is a guide to the eyes. The error bars represent uncertainties estimated by analyzing different EXAFS scans and considering correlations between different fit parameters.

Temperature dependence of h_z and α are shown in Fig. 5. The two parameters are correlated and they basically describe the same effect of the local bondings. Here, the anion height h_z is ~ 1.46 Å. Incidentally, the h_z is found to be ~ 1.47 Å in $\text{FeSe}_{1-x}\text{Te}_x$ with a negligible doping/temperature dependence^{22,23}. Therefore, the intercalation of ammonia seems to induce a compression of h_z . Also, the FT peaks (Fig. 2) at longer distances due to Fe-Fe correlations are much stronger in $\text{Li}_x(\text{NH}_3)_y\text{Fe}_2\text{Se}_2$ than in $\text{FeSe}_{1-x}\text{Te}_x$ system^{22,23}. This is an indication that the Fe-Fe layer in the ammonia intercalated system should be flatter than the one in the ternary $\text{FeSe}_{1-x}\text{Te}_x$. In addition,

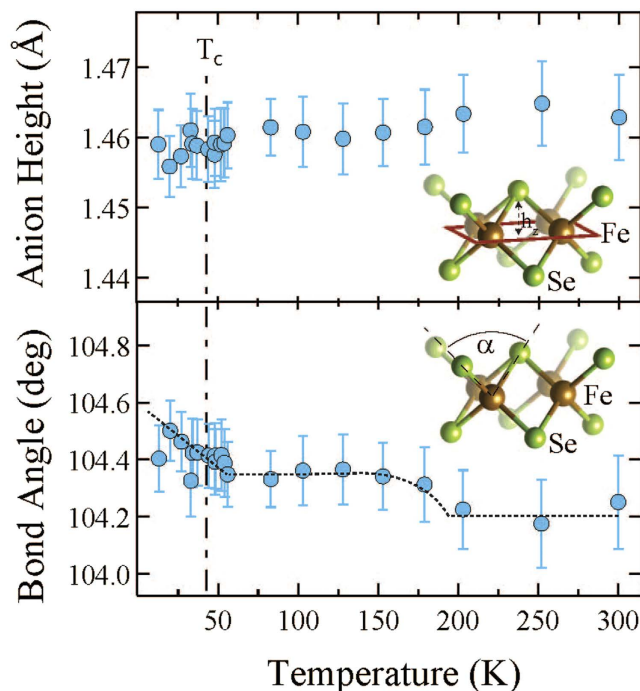


Figure 5. Temperature evolution of the local h_z and α parameters i.e. the Se-height from the Fe-Fe layer and the Se-Fe bond angle, respectively. These parameters are determined using the measured bond distances. Error bars take account of the correlations between the $R_{\text{Fe-Se}}$ and $R_{\text{Fe-Fe}}$ fit parameters. Cartoons showing definitions of the two parameters are also inserted. The dashed line in the lower panel is a guide to the eyes.

a small temperature dependent anomaly in h_z and α can be identified, revealing a slight increase in α (decrease of h_z) by cooling down across ~ 200 K and ~ 50 K. The freezing temperature for ammonia (NH_3) is ~ 195 K and it is possible that the change in the chalcogen height/bond angle at ~ 200 K to be due to a structural change in the intercalating layer, that may be affecting the local correlations of the active FeSe layer. A recent study has reported an anomaly in the quadrupole splitting ~ 240 K, measured by Mössbauer spectroscopy, and attributed this to a diffusive motion of Li^+ -ion within the spacer layers²⁴. Although, the small anomaly in the present work appears at a lower temperature, we can not rule out the small anomaly to be related with the Li^+ -ion motion, and more work is needed to establish the real cause. On the other hand, the anomaly ~ 50 K is likely to be related with the superconductivity at which the local Fe-Fe layer is getting thinner and flatter. These small changes can be better seen in the distance-distance correlations given by the σ^2 , measuring the MSRD.

The σ^2 is the second moment of the local bondlength distribution function and provides insight to the local bond dynamics. Figure 6 shows temperature dependence of σ^2 for the Fe-Se and Fe-Fe distances, obtained from Fe K-edge EXAFS analysis. The temperature dependence of $\sigma^2(T)$ can be described by the Einstein model^{20,25}

$$\sigma^2(T) = \frac{\hbar^2}{2k_B\mu\Theta_E} \coth\left(\frac{\Theta_E}{2T}\right) + \sigma_0^2 \quad (3)$$

where k_B is the Boltzmann constant, μ is the reduced mass of the considered absorber-backscatterer pair and σ_0^2 is a offset related with overall configurational disorder. Here, the $\sigma^2(T)$ for the two bondlengths is well described by the Einstein model down to the transition temperature T_c . However, at $T < T_c$ the σ^2 shows a down turn by cooling with a clear deviation from the Einstein-like behavior. Temperature dependent EXAFS permits to determine Einstein temperature Θ_E describing the bond stiffness. We have used the data between room temperature and ~ 50 K to determine Θ_E (see, e.g., model fits shown in Fig. 6). The Θ_E were found to be 313 ± 10 K and 248 ± 10 K respectively for the Fe-Se and Fe-Fe distances. These values are similar to the known values for the two bonds in the binary FeSe (~ 318 K and ~ 268 K^{22,23,26–28}). Thus, local bond correlations in $\text{Li}_x(\text{NH}_3)_y\text{Fe}_2\text{Se}_2$ are very similar to those in binary FeSe while ammonia intercalation seems to be separating the FeSe layers (increase of h_z), i.e., decoupling without any appreciable change in the local bond characteristics. It is worth mentioning that, while Θ_E for Fe-Se bonds in $\text{K}_x\text{Fe}_{2-y}\text{Se}_2$ also remains similar to the one in binary FeSe (and hence $\text{Li}_x(\text{NH}_3)_y\text{Fe}_2\text{Se}_2$), the Fe-Fe bond distance suffers a significant softening due potassium intercalation, with $\Theta_E \sim 200$ K^{26,27}.

Another important observation is the abrupt change in the σ^2 at $T \simeq T_c$. Such a change has been already observed in the atomic correlations measured in several superconductors^{29,30}. Here, the change in the σ^2 for Fe-Se bond is much smaller than that for the Fe-Fe bond. Earlier EXAFS studies on iron-based systems have pointed out such a change in the Fe-As correlations³¹, however, it turned out to be very small in the subsequent studies^{32,33}. The presence of this anomaly, indicating a local mode hardening by cooling across T_c , is a clear evidence of some correlation between electron-lattice interactions and superconductivity. The fact that such a local mode

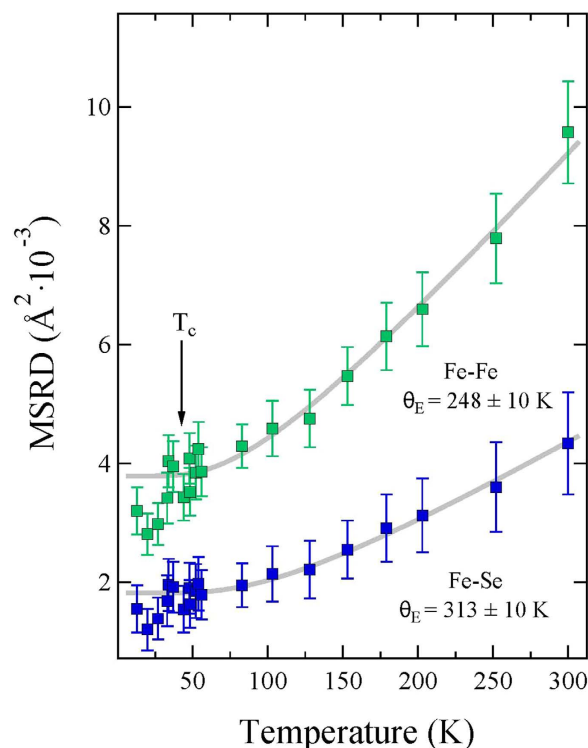


Figure 6. EXAFS Debye-Waller factors describing the mean square relative displacements (MSRD) as a function of temperature for the Fe-Se (blue squares) and Fe-Fe bonds (green squares). The Einstein model (3) fits are shown as grey solid lines.

hardening below T_c has been observed in different superconductors (e.g., cuprates³⁰, Nb₃Ge²⁹ and Fe-based materials), it is likely to be common feature of superconductivity phenomena. It should be mentioned that, for the cuprates the anomaly is associated with Cu-O bond correlations. Iron-based pnictides show anomaly to occur in Fe-Fe correlations while the Fe-As hardly showing such an anomaly³⁴. This may be related with the fact that the electronic states near the Fermi level in iron-based superconductors are mainly driven by Fe 3d orbitals with a limited contribution from the As p orbitals unlike the case of cuprates in which both Cu 3d and O 2p orbitals are strongly contributing. Incidentally, in the present work the anomaly appears not only in Fe-Fe but also the Fe-Se correlations, likely to be due to different anion chemistry in pnictides and chalcogenides. The fact that the anomaly is not always observed in iron-based systems it can be due to differences in their structural topologies and interlayer interactions depending on the kind of spacer layer. For example, REOFeAsO_{1-x}F_x (RE = rare-earth) system contains a well ordered REO spacer layer that may screen the anomaly at T_c unlike the systems in which the spacer is not well-defined. The BaFe₂As₂ is an example of the latter in which the anomalous change at T_c is well evident³⁴. Nevertheless, although the anomalous change across T_c suggests involvement of local lattice in the superconductivity, the question remains if this local lattice is directly causing the superconductivity (acting as a glue) or it is a mere consequence of the superconductivity phenomena, i.e., a transition from the incoherent local atomic correlations (in the normal state) to the coherent atomic correlations (in the superconducting state).

In summary, we have studied the local structure of superconducting Li_x(NH₃)_yFe₂Se₂ by means of in-plane polarized Fe K-edge EXAFS measurements performed on single crystal samples. We find that the Se-height from the Fe-Fe layer, determined by the direct measurements of Fe-Se and Fe-Fe bond lengths, appears shrunk in the intercalated system with respect to the binary FeSe. In addition to the compressed FeSe₄ tetrahedron, the results reveal that the bond length characteristics, measured by the temperature dependence of the mean square relative displacements, hardly show any effect of the molecular layer intercalation. On the other hand, the local structure response to the superconductivity appears as an anomalous change in the MSRD across the superconducting transition temperature T_c , an indication of a sudden change in the atomic correlations in the superconducting phase. It is argued that the higher T_c of the ammonia intercalated system should be related with an effective compression of the FeSe-layers (with flatter Fe-Fe layer) and interlayer decoupling due to a thick spacer layer. Nevertheless, the results underline importance of the local atomic correlations in the superconductivity of these materials.

Methods

Sample synthesis and characterization. Single crystal samples of Li_x(NH₃)_yFe₂Se₂ were synthesized using liquid ammonia as a solvent. Several single crystals of FeSe and dopant metal in the appropriate ratio were placed in a glass tube. NH₃ gas was condensed in the glass tube by cooling with liquid N₂. The glass tube was filled with liquid NH₃ (~10 ml) and was sealed. After the intercalation reaction, the liquid NH₃ was removed by heating

and dynamically pumping the glass tube, finally obtaining metal-doped single crystals. The samples were handled in a glove box ($O_2 \leq 0.5$ ppm and $H_2O \leq 0.5$ ppm). The samples were characterized by in-house X-ray diffraction (XRD) from the basal plane of single crystals of parent FeSe and $Li_x(NH_3)_yFe_2Se_2$ using a RIGAKU Ultima IV at room temperature with Co source ($\lambda = 1.79 \text{ \AA}$). The structural parameters obtained on the single crystal samples studied in the present work are consistent with those reported for polycrystalline samples⁶. The *c*-axis of the intercalated sample was found to be 17.24 \AA for I4/mmm structure. The magnetization measurements were carried out using a SQUID magnetometer (MPMS-R2 and MPMS3, Quantum Design Co. Ltd.). The temperature dependent resistivity was measured using a Physical Properties Measurement System (PPMS, Quantum Design Co. Ltd. with magnetic field up to 9 Tesla). The quantitative composition of the samples was determined by analyzing energy dispersive x-ray (EDX) spectra obtained with a VE-9800SP (Keyence Co. Ltd.) equipped with a scanning electron microscope (SEM). The EDX spectra were obtained from the cleaved surfaces of single crystals of $Li_x(NH_3)_yFe_2Se_2$. Li and NH_3 concentrations were determined by analyzing inductively coupled plasma (ICP) atomic emission spectroscopy (Vista-pro, Seiko Instruments Co. Ltd.), and found to be $x \sim y \sim 0.11$ for the samples used in the present study.

X-ray absorption measurements. Single crystal samples were used for the EXAFS measurements. Temperature dependent x-ray absorption measurements were carried out at the CLÆSS beamline of the ALBA synchrotron in Cerdanyola del Valles (Barcelona) where the synchrotron radiation emitted by a multipole wiggler was monochromatized by a Si(111) double crystal monochromator and Rh-coated mirrors were used to reject higher harmonics. Due to the alkali-metal content, the samples are prone to degradation if placed in ambient atmosphere. To avoid degradation, all the preparation procedures were performed in glovebox under Ar atmosphere, samples were then transferred to the measurement stage. The samples were exfoliated for transmission measurements to reach the desired thickness for absorption jump to be ~ 1 at the Fe K-edge energy (7112 eV). The absorption experiments were carried out in the normal incidence geometry exploiting three ionization chambers mounted in series to measure the energy-dependent absorption coefficient of the sample and a reference Fe-foil at the same time. In the geometry the polarization of the x-ray beam is parallel to the *ab*-plane of the single crystal samples. Samples were mounted on a cold finger attached to a Helium cryostat and measured in the temperature range of $13\text{--}300 \text{ K}$. The sample temperature was maintained within $\pm 0.5 \text{ K}$ during each data acquisition. Several scans were collected for any given temperature to ensure reproducibility and improve the signal-to-noise ratio.

References

- Mizuguchi, Y. & Takano, Y. Review of Fe Chalcogenides as the Simplest Fe-Based Superconductor. *J. Phys. Soc. Jpn.* **79**, 102001 (2010).
- Mizuguchi, Y., Tomioka, F., Tsuda, S., Yamaguchi, T. & Takano, Y. Superconductivity at 27 K in tetragonal FeSe under high pressure. *Appl. Phys. Lett.* **93**, 152505 (2008).
- Guo, J. *et al.* Superconductivity in the iron selenide $K_xFe_2Se_2$ ($0 \leq x \leq 1.0$). *Phys. Rev. B* **82**, 180520(R) (2010).
- Ying, J. J. *et al.* Superconductivity and magnetic properties of single crystals of $K_{0.75}Fe_{1.66}Se_2$ and $Cs_{0.81}Fe_{1.61}Se_2$. *Phys. Rev. B* **83**, 212502 (2011).
- Dagotto, E. Colloquium: The unexpected properties of alkali metal iron selenide superconductors. *Rev. Mod. Phys.* **85**, 849 (2013).
- Burrard-Lucas, M. *et al.* Enhancement of the superconducting transition temperature of FeSe by intercalation of a molecular spacer layer. *Nat. Mat.* **12**, 15 (2012).
- Izumi, M. *et al.* Emergence of double-dome superconductivity in ammoniated metal-doped FeSe. *Sci. Rep.* **5**, 9477 (2015).
- Zheng, L. *et al.* Emergence of Multiple Superconducting Phases in $(NH_3)_MFeSe$ (M: Na and Li). *Sci. Rep.* **5**, 12774 (2015).
- Guo, J., Lei, H., Hayashi, F. & Hosono, H. Superconductivity and phase instability of NH_3 -free Na-intercalated $FeSe_{1-x}S_x$. *Nat. Comm.* **5**, 4756 (2014).
- Dong, X. *et al.* Phase Diagram of $(Li_{1-x}Fe_x)OHFeSe$: A Bridge between Iron Selenide and Arsenide Superconductors. *J. Am. Chem. Soc.* **137**, 66 (2015).
- Sun, H. *et al.* Soft Chemical Control of Superconductivity in Lithium Iron Selenide Hydroxides $Li_{1-x}Fe_x(OH)Fe_{1-y}Se$. *Inorg. Chem.* **54**, 1958 (2015).
- Hayashi, F., Lei, H., Guo, J. & Hosono, H. Modulation Effect of Interlayer Spacing on the Superconductivity of Electron-Doped FeSe-Based Intercalates. *Inorg. Chem.* **54**, 3346 (2015).
- Yusenko, K. V. *et al.* Hyper-expanded interlayer separations in superconducting barium intercalates of FeSe. *Chem. Commun.* **51**, 7112 (2015).
- Ge, J.-F. *et al.* Superconductivity above 100 K in single-layer FeSe films on doped $SrTiO_3$. *Nat. Mat.* **14**, 285 (2015).
- Mizukami, Y. *et al.* Disorder-induced topological change of the superconducting gap structure in iron pnictides. *Nat. Comm.* **5**, 5657 (2014).
- Mizuguchi, Y. *et al.* Anion height dependence of T_c for the Fe-based superconductor. *Supercond. Sci. Technol.* **23**, 054013 (2010).
- Kuroki, K., Usui, H., Onari, S., Arita, R. & Aoki, H. Pnictogen height as a possible switch between high- T_c nodeless and low- T_c nodal pairings in the iron-based superconductors. *Phys. Rev. B* **79**, 224511 (2009).
- Bunker, G. *Introduction to XAFS*, Cambridge University Press, 2010; see also *X-ray Absorption: Principles, Applications, Techniques of EXAFS, SEXAFS, XANES*, edited by R. Prins & D. C. Koningsberger (Wiley, New York, 1988).
- Ravel, B. & Newville, M. ATHENA, ARTEMIS, HEPHAESTUS: data analysis for X-ray absorption spectroscopy using IFEFFIT. *J. Synch. Rad.* **12**, 537 (2005).
- Rehr, J. J. & Albers, R. C. Theoretical approaches to x-ray absorption fine structure. *Rev. Mod. Phys.* **72**, 621 (2000).
- Lee, P. A., Citrin, P. H., Eisenberger, P. & Kincaid, B. M. Extended x-ray absorption fine structure - its strengths and limitations as a structural tool. *Rev. Mod. Phys.* **53**, 769 (1981).
- Joseph, B. *et al.* Evidence of local structural inhomogeneity in $FeSe_{1-x}Te_x$ from extended x-ray absorption fine structure. *Phys. Rev. B* **82**, 020502 (2010).
- Iadecola, A. *et al.* Random alloy-like local structure of $Fe(Se, S)_{1-x}Te_x$ superconductors revealed by extended x-ray absorption fine structure. *J. Phys. Condens. Matter* **23**, 425701 (2011).
- Shylin, S. I. *et al.* Intercalation effect on hyperfine parameters of Fe in FeSe superconductor with $T_c = 42 \text{ K}$. *EPL* **109**, 67004 (2015).
- Sevillano, E., Meuth, H. & Rehr, J. J. Extended x-ray absorption fine structure Debye-Waller factors. I. Monatomic crystals. *Phys. Rev. B* **20**, 4908 (1979).
- Iadecola, A. *et al.* Large local disorder in superconducting $K_{0.8}Fe_{1.6}Se_2$ studied by extended x-ray absorption fine structure. *J. Phys. Condens. Matter* **24**, 115701 (2012).

27. Iadecola, A. *et al.* Local structure response of phase separation and iron-vacancy order in $K_xFe_{2-y}Se_2$ superconductor. *Phys. Rev. B* **90**, 174509 (2014).
28. Tyson, T. A. *et al.* Local structure of the superconductor $K_{0.8}Fe_{1.6+x}Se_2$: Evidence of large structural disorder. *Phys. Rev. B* **85**, 024504 (2012).
29. Saini, N. L. *et al.* Temperature-dependent local structure in the Nb_3Ge superconductor studied by high-resolution Ge K-edge EXAFS measurements. *Phys. Rev. B* **68**, 104507 (2003).
30. Saini, N. L., Bianconi, A. & Oyanagi, H. Evidence for Critical Lattice Fluctuations in the High Tc Cuprates. *J. Phys. Soc. Jpn.* **70**, 2092 (2001).
31. Zhang, C. J., Oyanagi, H., Sun, Z. H., Kamihara, Y. & Hosono, H. Electronic and lattice structures in $SmFeAsO_{1-x}F_x$ probed by x-ray absorption spectroscopy. *Phys. Rev. B* **81**, 094516 (2010).
32. Joseph, B., Iadecola, A., Malavasi L. & Saini, N. L. Temperature-dependent local structure of $NdFeAsO_{1-x}F_x$ system using arsenic K-edge extended x-ray absorption fine structure. *J. Phys.: Condens. Matter* **23**, 265701 (2011).
33. Joseph, B. *et al.* Temperature dependent local atomic displacements in Ru substituted $SmFe_{1-x}Ru_xAsO_{0.85}F_{0.15}$ superconductors. *Supercond. Sci. Technol.* **26**, 065005 (2013).
34. Hacisalihoglu, M. Y. *et al.* A study of temperature dependent local atomic displacements in a $Ba(Fe_{1-x}Co_x)_2As_2$ superconductor. *Phys. Chem. Chem. Phys.* **18**, 9029 (2016).

Acknowledgements

We thank ALBA staff for the assistance during the measurements. One of us (T.W.) would like to acknowledge hospitality at the Sapienza University of Rome. This research was partially supported by the Program for Promoting the Enhancement of Research University from MEXT and the Program for Advancing Strategic International Networks to Accelerate the Circulation of Talented Researchers from JSPS. The support from the Grant-in-Aid for Scientific Research from the Japan Society for the Promotion of Science coordinated by M. Nohara (26287082 and 15H05886), K. Kudo (25400372 and 15H01047), by T. Kambe (15H03529) is acknowledged. The work is a part of the executive protocol of the general agreement for cooperation between the Sapienza University of Rome and the Okayama University, Japan. The work at Sapienza is partially supported by PRIN2012 (grant number 2012X3YFZ2) of MIUR, Italy.

Author Contributions

N.L.S., T.Y., T. Kambe and M.N. programmed and coordinated the study. J.-H.L., T. Kakuto, N.N., T. Kimura, K.K., T. Kambe and M.N. have synthesized the single crystals used for the study. E.P., L.S., T.W., C.M., W.O. and N.L.S. performed the experiments at the CLAES beamline of the ALBA synchrotron facility and contributed in the data analysis. N.L.S., T.Y., T. Kambe, T.W. and K.T. were part of the scientific discussions on the analysis and interpretations. E.P. and N.L.S. wrote the preliminary draft of the manuscript that was discussed by all the authors to produce the final draft with key inputs from T. Kambe and T.Y.

Additional Information

Competing financial interests: The authors declare no competing financial interests.

How to cite this article: Paris, E. *et al.* Temperature dependent local atomic displacements in ammonia intercalated iron selenide superconductor. *Sci. Rep.* **6**, 27646; doi: 10.1038/srep27646 (2016).



This work is licensed under a Creative Commons Attribution 4.0 International License. The images or other third party material in this article are included in the article's Creative Commons license, unless indicated otherwise in the credit line; if the material is not included under the Creative Commons license, users will need to obtain permission from the license holder to reproduce the material. To view a copy of this license, visit <http://creativecommons.org/licenses/by/4.0/>